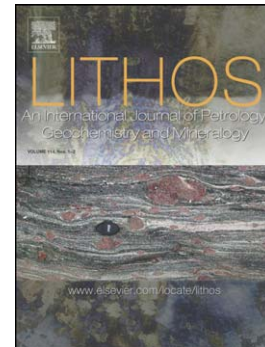# Accepted Manuscript

Geochemical stratigraphy and correlation within Large Igneous Provinces: The final preserved stages of the Faroe Islands Basalt Group

J.M. Millett, M.J. Hole, D.W. Jolley, S.R. Passey

Please cite this article as: Millett, J.M., Hole, M.J., Jolley, D.W., Passey, S.R., Geochemical stratigraphy and correlation within Large Igneous Provinces: The final preserved stages of the Faroe Islands Basalt Group, *LITHOS* (2017), doi:10.1016/j.lithos.2017.05.011

Geochemical stratigraphy and correlation within Large Igneous Provinces: the

final preserved stages of the Faroe Islands Basalt Group

J.M. Millett[1,2]*, M. J. Hole[2], D.W. Jolley[2], S.R. Passey[3]

[1]*VBPR AS, Oslo Science Park, Gaustadalléen 21, N-0349 Oslo, Norway*

[2]*Department of Geology & Petroleum Geology University of Aberdeen, AB24 3UE, Scotland*

[3]*CASP, West Building, 181A Huntingdon Road, Cambridge CB3 0DH, UK*

*Corresponding author email: john.millett@abdn.ac.uk*

**Abstract**

*The Faroe Islands Basalt Group (FIBG) comprises a gross stratigraphic thickness of over 6.5 km of dominantly extrusive basaltic facies erupted during the Late Palaeocene to Early Eocene. In this study we present 140 major and trace element analyses from flow by flow field and borehole sample profiles, through the Enni Formation, which comprises the final phase of volcanism preserved on the Faroe Islands. The sample profiles target geographically spaced and overlapping stratigraphic sequences tied relative to a 3D ArcGIS surface for the regionally extensive volcaniclastic Argir Beds marker unit. From these profiles five geochemical groups including one low $TiO_2$ (Low-Ti <1.5 wt %) and four high $TiO_2$ (High-Ti >1.5 wt %) groups differentiated by Nb, Zr, Y and V variations are identified in conjunction with previous studies. The spatial and stratigraphic distribution of these groups is mapped across the islands and demonstrates a complex inter-digitated flow field evolution. Within the finer scale variations, broad spatial and temporal development trends are identified demonstrating the potential for correlation within the volcanic succession at the local, tens of kilometres scale. Low-Ti lavas formed in association with lithospheric thinning and developed extensive flow fields between the Faroe Islands and East Greenland contemporaneous to the eruption of High-Ti smaller melt fraction lava flows in both locations. The progression of High-Ti lava groups preserved on either side of the developing rift zone is very similar, but is not, however, chronostratigraphic due to multiple inter-digitations of the chemical types. We tentatively suggest that a previously proposed rift-oblique transfer zone between the Faroe Islands and East Greenland enabled non-uniform lithospheric thinning and the preservation of a near-continuous High-Ti melting region between these areas beyond the onset of Low-Ti eruptions which were initially fed from the west. This study highlights the complex nature of late stage flood basalt plumbing systems and eruption dynamics in a rift proximal setting.*

**Introduction**

The Faroe Islands are situated in the North Atlantic Ocean between the UK and Iceland, (Fig. 1). The islands are composed entirely of the exposed remnants of the extensive lava plateau of the Palaeogene Faroe Islands Basalt Group (FIBG, Passey and Jolley, 2009), part of the larger North Atlantic Igneous Province (NAIP, Saunders et al., 1997). The majority of the FIBG comprises subaerial lava flows interbedded with pyroclastic and sedimentary (interbed) facies of much smaller volumes (Rasmussen and Noe-Nygaard 1970, Waagstein 1988, Passey and Bell 2007, Passey and Jolley 2009). The islands, along with their surrounding shallow shelf, comprise the Faroe Platform, a partly subsided section of the NW European continental margin (Waagstein 1988). Based on geophysical data, the Faroe Islands are inferred to be underlain by 35-40 km thick cratonic basement connected to the UK continental shelf (Bott *et al.,* 1974; Casten 1973; Richardson *et al.,* 1999). Isotopic evidence for contamination of some lava flows by Precambrian amphibolite facies also supports the presence of continental crust beneath the islands (Gariepy *et al.,* 1983; Hald & Waagstein 1983; Holm *et al.,* 2001) although contamination is generally very minor (Holm *et al.,* 2001).

A striking feature of the FIBG is the correspondence that has been identified between lava geochemical stratigraphic cycles, interbed development and ecosystem dynamics within the older Beinisvørð and Lopra Formations (Jolley *et al.* 2012). These magmatic cycles comprise initial mafic magma pulses followed by progressively more fractionated sequences, which are accompanied by interbed ecological signatures for increasing inter-eruption hiatus lengths towards the end of each cycle. This relationship, however, breaks down in the younger Malinstindur and Enni Formations, which comprise a mixed sequence of simple and compound lava flow facies with generally very minor volcaniclastic intercalations (Passey & Bell 2007; Passey & Jolley, 2009). The breakdown in this relationship is accompanied by the presence of separate low and high $TiO_2$ lava geochemical groups in the upper Malinstindur and Enni Formations (Waagstein 1988). Published stratigraphically constrained geochemical data for the

Enni Formation is presented by (Rasmussen & Noe-Nygaard, 1969; Søager & Holm, 2009, 2011) with further spot sample analyses being published by Waagstein (1977) and Hald & Waagstein (1983).

Differentiation of the broad geochemical groups of the FIBG was defined using a classification scheme by Waagstein (1988) in which major groups from the FIBG were separated on a plot of $TiO_2/FeO_t$ versus $FeO_t/MgO$ (Waagstein 1988; Larsen et al., 1999). The low $TiO_2$ compositions, recognised as MORB-like by Waagstein (1988), are proposed to have been sourced from the incipient rift zone to the north of the Faroe Islands at the time. These groups were investigated in more detail by spot sampling across the islands where one low $TiO_2$ group (Low-Ti <1.5 wt %) and three high $TiO_2$ groups (High-Ti1, 2 & 3 all >1.5 wt %) were identified based on trace element and isotopic constraints (Søager & Holm, 2009).

This study focuses on the spatial and temporal development of lava geochemical groups within the youngest Enni Formation lava flows of the FIBG on the Faroe Islands. The bio-stratigraphic and isotopic corroborated age of the Enni Formation is c. 55 Ma (Jolley et al., 2002; Storey et al., 2007; Passey & Jolley 2009). The formation, along with the underlying Malinstindur Formation, comprises the syn-breakup sequence of the NAIP (Larsen et al., 1999; Jolley & Bell 2002; Storey et al., 2007). Within the Enni Formation, the laterally extensive volcaniclastic dominated Argir Beds (Fig. 1d) form an important stratigraphic marker unit (Passey & Jolley 2009, Passey & Varming 2010). All samples in this study are therefore presented relative to the GIS surface for the Argir Beds (Passey & Varming, 2010). Through detailed zeolite zone mapping of the FIBG it has been estimated that around c. 1 km of stratigraphy is missing from the top of the Faroe Islands due to erosion (Jørgensen, 1984; Waagstein *et al.*, 2002; Jørgensen 2006). Therefore, although this study investigates the uppermost preserved stratigraphy, the last eruptive products on the islands no longer exist due to erosion, so we are investigating the late stages, but not final eruptions of the FIBG.

Understanding the temporal and spatial evolution of LIP sequences is not only important for building our understanding of these major episodes in earth history, but also has significant practical applications. For correlation within LIP deposits, these applications are far reaching and include sub-surface exploration for hydrology (Burns *et al.* 2012), geothermal energy (Fridleifsson & Elders 2005), petroleum resources (Jerram, 2015; Millett et al., 2015) along with the potential for $CO_2$ sequestration (Zakharova *et al.,* 2012) and natural gas storage (Reidel *et al.,* 2002). Understanding the potential but also the limitations of geochemical correlation within LIP sequences is therefore important for the effective exploration and development of resources associated with LIPs.

**Methods**

Several overlapping stratigraphic sample profiles were collected through the Enni Formation for this study. Every individual flow along a stratigraphic profile was sampled within the constraints of exposure and access. This involved, in a number of cases, sampling flows that were extensively altered or highly amygdaloidal. We justify sampling such flows due to the immobile behaviour of elements key to petrogenetic discrimination, such as Ti, P, Zr, Y and Nb, during pedogenesis and low grade metamorphism of basalts (e.g. Babechuk *et al.* 2014; Morrison 1978) along with the infinitely greater uncertainty of not sampling such stratigraphic intervals. For each sampled section (see supplementary data) the vast majority of flows were sampled, but where omissions occurred these are recorded in the presented stratigraphic columns. Sampling of altered compound flows was undertaken according to thickness, exposure and the presence of definite flow boundaries. Where substantial thicknesses occurred e.g. >10 m then a sample was generally taken from the base and from the top of the sequence. Sampling of tabular flows was undertaken from the freshest accessible part of each flow.

All GPS points were taken in the European Datum 1950 (ED50) coordinate system (same as the presently available topographic maps for the islands) in decimal degrees using a Garmin Etrex Legend HCX handheld GPS receiver with typical horizontal accuracy of c. 3 m. The elevations for all waypoints were later extracted from the high resolution Digital Elevation Model (DEM) of the Faroe Islands in ArcGIS. The Argir Beds stratigraphic marker unit from the FIBG digital framework (Passey & Jolley, 2009; Passey & Varming, 2010) was used for relative height extraction and correlation in this study. The base of the Argir Beds forms a lithohorizon that has been mapped across the islands (Passey & Varming 2010) and is treated here, as a broadly isochronous surface. Minor updates to the Argir Beds surface were made using the spline surface interpolation tool in ArcGIS to incorporate additional reference points (Millett, 2014).

140 basalt samples were analysed for major and trace elements by XRF on an ARL 8420+ dual goniometer wavelength dispersive XRF spectrometer at the Open University. Samples were first crushed by fly-press followed by powdering of the least altered rock chips minus any observed secondary amygdale material in an Agate tema mill at the University of Aberdeen. Major elements were determined on fused glass beads prepared from ignited powders mixed with a lithium metaborate/tetraborate flux following the analytical procedures outlined in Ramsey *et al.* (1995). In-house standards (WS-E & OU-3) were run at regular intervals to ensure analytical precision and accuracy (see supplementary data). Loss on ignition was determined after heating to 1000°C. Loss on ignition (LOI) ranges from c. 0 to 6.7 % for the dataset with the majority of samples (122 of 140) displaying values <3 % with a positive skew towards zero. It is noted that the oxidation of FeO to $Fe_2O_3$ during ignition means that the reported LOI values will be slightly underestimated where original FeO values were near c. 10 % for many of our samples. Trace elements were analysed on pressed powder pellets prepared after the method of (Watson 1996). Reference standards (BHVO-1, DNC-1, QLO-1 & W-2) were run at regular intervals to ensure analytical accuracy (see supplementary data).

Rare Earth Elements (REEs) were analysed by ICP-MS on an Agilent 7500s ICP-MS machine at the Open University on a subset of 34 samples selected based on the XRF results. The analyses were run calibrated against the reference materials set (BIR-1, BHVO-2, W-2, DNC-1 and AGV-1) to monitor accuracy and precision (see supplementary data). Mineral chemistry data was acquired on a MICROSCAN MK5 using a Link Analytical AN10/25S system at the University of Aberdeen. Data was acquired and processed using the ZAF4/FLS program.

**Stratigraphic Profiles**

Samples were collected from seven stratigraphic profiles and from three broad areas of the exposed Enni Formation (Figs. 1 and 2). The three areas comprise thick packages of Enni Formation lava flows and will be referred to in the text as the NE islands (Viðoy and Svínoy), the central islands (including Streymoy, Nólsoy and the southern tip of Eysturoy), and Sandoy (the southernmost exposures of the Enni Formation investigated in this study), see Figure 2. In all three areas sampling was undertaken from, or just below, the Argir Beds reference surface upwards, and include the youngest Enni Formation lavas exposed in each region aside from in the northeast where slightly younger lavas may be exposed on Fugloy (Passey, 2009, Passey & Jolley, 2009; Passey & Varming, 2010). All samples were collected from surface exposures aside from the basal part of the Nólsoy sequence, which comprises a compiled stratigraphic section (including whole rock geochemistry) from a suite of four shallow boreholes (Jolley & Passey, 2013). In all three areas sample profiles were chosen to overlap in relation to the 3D spatial framework so that continuous compiled sections through the Enni Formation could be investigated within each.

The lava flow facies within the Enni Formation comprise interdigitating simple (tabular) and compound (braided) lava flows, often forming packages of a few tens to hundreds of metres (Passey & Bell, 2007; Passey & Jolley, 2009). Flow crusts are invariably

deeply weathered and in general the compound lava flows are more weathered than the simple flows due to their higher initial vesicularities and larger crust/core ratios (Fig. 3). In most cases, flow boundaries are weakly to pervasively oxidized with thin reddened boles and volcaniclastic units occurring between some flow packages (Fig. 3). Initial vesicular pore spaces within the sampled lavas have predominantly been filled with various zeolites, calcite and clays although partially filled and unfilled vesicles are also present in places (Jørgensen, 1984; Jørgensen, 2006).

The sampled lava flows comprise finely crystalline aphyric to plagioclase, olivine and much less commonly augite porphyritic basalts (Fig. 2). In general, the Low-Ti group lavas display aphyric to sparsely olivine and plagioclase phyric textures. Olivine is largely absent from the High-Ti lava flows, which are more commonly plagioclase phyric to aphyric. The High-Ti lava flows may also be densely plagioclase phyric in some cases with large zoned glomerocrysts displaying partially resorbed sieve textures indicative of disequilibrium. Groundmass textures range from inter-granular to intersertal with ophitic textures also occurring in a number of samples.

**Geochemistry**

*Alteration*

High LOI values are exclusively associated with the previously discussed deeply weathered samples and therefore, the likelihood of post-emplacement redistribution of the more mobile major and trace elements is increased for these samples. Mobile elements such as Sr and Na display only limited additional scatter when compared to immobile elements such as Zr for the higher LOI samples, however, K displays clearly increased scatter, (Fig. 4), a common feature of similar aged basalts from East Greenland (e.g. Larsen et al., 1989). In contrast, the immobile elements such as Zr, Ti and P (all incompatible with early crystallizing

phases in basaltic melts) show strong linear correlations irrespective of LOI confirming a lack of any redistribution of these elements during post emplacement alteration (Fig. 4). All plotted major element data are recalculated to 100 wt. % on a dry basis with a fixed oxidation ratio of $Fe_2O_3/FeO = 0.15$ as used by Larsen et al. (1999) for basalts of the FIBG.

*Crystal accumulation*

A number of samples display combined chemical and petrographic evidence for plagioclase accumulation. High $Al_2O_3$ samples (>15.5 wt. % used for the similar aged successions on East Greenland, Larsen *et al.* 1989), plot along mixing lines between aphyric sample compositions and average plagioclase phenocryst compositions (e.g. $An_{70}$, Millett, 2014) from the Enni Formation (Fig. 4). These accumulation trends also potentially extend below 15.5 wt. % $Al_2O_3$ for the more evolved compositions (Fig. 4). High MgO samples are predominantly associated with Low-Ti compositions and lie along mafic olivine (e.g. $Fo_{85}$) control lines (Fig. 5). Glomerocrysts of olivine in some samples suggest minor accumulation effects, however, due to the weakly olivine porphyritic textures of most high MgO samples, olivine fractionation is inferred as the dominant MgO control for these samples.

*Crustal contamination*

Ratios of incompatible elements such as Ba/Nb, Ba/Th and Ba/Zr have been found to closely relate to isotopic (Sr-Nd and Pb-Pb) signatures for crustal contamination of NAIP magmas (Kerr, 1995; Larsen et al., 1998; Fitton et al., 1998; Holm et al., 2001; Kent et al., 2002). In this study, no isotopic data is available and so the trace element ratios Ba/Zr and $La/Nb_N$ (normalized to primitive mantle, McDonough & Sun 1995) are used to assess crustal contamination. Ba/Zr values >1-2 or La/Nb >1.5 may suggest possible crustal contamination (Larsen et al., 1998; Holm et al., 2001). Evidence for crustal contamination is very limited,

with all except four samples displaying Ba/Zr < 1, normal $SiO_2$ (Fig. 4) and $La/Nb_N$ < 1.5 (not shown). The four samples displaying slightly elevated values are still low in comparison to the values observed in ODP Legs 152 and 163 from the SE Greenland margin (Larsen et al., 1998; Fitton et al., 1998) and are well within the array displayed by the Site 917 Upper series, which are regarded as relatively uncontaminated. Samples showing elevated silica and increased levels of crustal contamination are found on the Faroe Islands (e.g. Hald & Waagstein, 1983), however, these are volumetrically very restricted.

### *Lava group subdivisions*

Only samples with LOI < 3 wt.%, Ba/Zr < 1 and $Al_2O_3$ < 15.5 wt. % are presented in this section to avoid any unquantified effects relating to alteration, contamination and crystal accumulation. All Enni Formation lavas comprise basaltic compositions (TAS classification of Le Maitre et al. 1989) of exclusively tholeiitic affinity (AFM scheme of Irvine & Barager, 1971) which are features common to the entire FIBG (Waagstein, 1988; Passey & Jolley, 2009).

Two major groups including a low $TiO_2$ ($TiO_2$ <1.5 wt. %) and high $TiO_2$ ($TiO_2$ >1.5 wt. %) series are clearly defined from major element compositions alone (Fig. 5). The Low-Ti group comprises a less evolved suite of basalt with a wide range of MgO from c. 6.8 to 13.1 wt.% whereas the High-Ti lava flows are much more evolved occupying a range of MgO from c. 5.7 to 7.3 wt.% MgO. The Low-Ti suite is dominated by an olivine fractionation trend above Mg# c. 58 (MgO c. 9 wt.%), below which point a clear inflection in the plots of FeOt, $Al_2O_3$ and CaO occurs signalling the onset of plagioclase +/- clinopyroxene crystallization (Fig. 4 and 5, see also Søager & Holm, 2011). Major element variations between the High-Ti Enni Formation samples are less systematic, however, they may be further subdivided into four sub groups (High-Ti1, -2, -3 and -4) based on incompatible and

immobile trace element criteria (Fig. 6). These groupings are largely comparable with and can be related to the nomenclature of Søager & Holm (2009) with the addition of a new subgroup (High-Ti4) for which only a single sample (Sample 121606 of Søager & Holm, 2009) has previously been reported. The geochemical groups are defined in Table 2 (after Millett, 2014) based on chemical criteria alone without reference to stratigraphic position.

In Figure 6, lines of constant inter-element ratios intersecting the origin have been plotted to intersect the main group arrays. Low-Ti lava flows display a very distinct Zr/Y ratio of c. 2.27, much lower than any of the high TiO$_2$ groups. The ratios of Zr/Nb c. 22.8 and Nb/Y c. 0.1 are also distinct from the other groups but are, however, more scattered due to the low absolute values of Nb within the group which is close to the detection limit of the XRF analytical determination.

In general, the high TiO$_2$ groups display strong linear arrays of incompatible trace elements with the High-Ti3 lavas displaying the greatest scatter on all diagrams in comparison to the other groups. The Zr/Y ratio of c. 5.4 for the High-Ti3 lavas is indistinguishable from the High-Ti1 lavas, but the Zr/Nb and Nb/Y ratios for High-Ti3 lavas are distinct from High-Ti2 lavas and display minor overlap with High-Ti4 lavas. The scatter in the data cannot be explained by simple upper crustal magma chamber processes from a single source and so some degree of mixing or source variation must be invoked for the group. High-Ti3 and High-Ti4 lavas overlap in all but the V versus Nb/Y plot in Figure 6. The clear separation between High-Ti3 and High-Ti4 lava flows based on High-Ti4 lavas relative enrichment in V (along with TiO$_2$, FeO$_t$, Zn etc. not shown) at overlapping values of incompatible element ratios suggests that the High-Ti4 lavas comprise a distinct melt batch which does not appear to be related to High-Ti3 or any other group by shallow magma chamber dynamics involving any of the observed phenocryst phases. The cause of this enrichment in High-Ti4 lavas remains poorly constrained, however, the clear stratigraphic association of this flow

package along with the REE evidence for slightly larger and shallower degrees of melting compared to High-Ti3 lavas, discussed below, support them forming a distinct magma batch.

Figure 7(a) displays representative REE element data for the separate groups. The Low-Ti magmas display distinctly LREE depleted signatures e.g. La/Sm$_N$ <1 similar to modern day MAR N-MORB (e.g. Debaille et al., 2006) and the more enriched High-Ti groups display LREE enriched signatures La/Sm$_N$ >1 more similar to E-MORB. The data are compared to simple non-modal incremental batch melting models in Figure 7(b), which clearly displays the Low-Ti magma suite must have been generated from a depleted mantle source (e.g. Waight & Baker, 2012). This is in contrast to the High-Ti groups that must have been generated from a significantly more enriched source composition. Absolute values of the degree and depth of melting are highly model dependent. However, within a range of realistic starting compositions and modelling parameters it is apparent that a proportion of melting for both the Low-Ti and High-Ti suites likely took place within the garnet stability field of the mantle. This therefore implies elevated temperatures and at least some melting >2.7 GPa. The High-Ti groups all display very similar REE patterns, but plot as separate groups on the melting diagram albeit within a relatively very tight overall range. In general, the High-Ti1 and High-Ti2 groups display tendencies to slightly larger melt fractions (lower La/Yb$_N$) along with stronger garnet signatures (at higher Dy/Yb$_N$) compared to the High-Ti3 and High-Ti4 groups.

The REE element data for the separate groups correspond well to the data from Søager & Holm (2009; 2011) and therefore, their isotopic arguments for the separate mantle source components of the separate Enni Formation groups can reasonably be extended to the sub-group data in this study. This infers that although the High-Ti groups are very similar on the basis of many chemical criteria, that they also comprise distinct and coherent magmatic batches coming from depth and which erupted at the surface as distinct petrogenetic suites. This assessment, if correct, therefore enables the detailed mapping of these chemical units within the late stages of

the FIBG lava pile to assess when, where and how these melt batches were fed onto the FIBG palaeo-surface during the last stages of the syn-rift volcanism.

A small group of samples have been termed 'Transitional' due to their plotting as outliers between the main groups and can reasonably be explained by mixing lines between the Low-Ti and High-Ti suites suggesting that sub-surface mixing of contemporaneous magma batches occurred (e.g. Millett, 2014). The Transitional lava flows show greatest affinity to the Low-Ti suite based on major elements and therefore it appears likely that they derived their mixed trace element signatures by interaction of a Low-Ti melt with a smaller volume of more trace-element enriched High-Ti melts. Two additional samples display no clear affinity with any of the groups and are simply labelled undefined within the supplementary data.

Samples initially screened out as having high LOI, high $Al_2O_3$ or evidence for contamination, were subsequently assessed in light of the above chemical groups. A number of these samples remain undefined, but where any of these samples fits with all of a groups criteria, they have been labelled as relating to the respective group with the qualifier high LOI, high Al or contaminated, noted in brackets (supplementary data).

**Geochemical stratigraphy and correlation**

The compiled geochemical and facies stratigraphic profiles are combined and presented in the correlation panel in Figure 8. Dashed tie lines have been added to the section to represent a potential correlation framework that honours all the available spatially constrained geochemical data within this study. The presented tie line correlations are non-unique but form a best estimate; in all cases the simplest scenario for joining the chemical profiles was sought. In many cases, individual lava flows with a distinct chemical signature are found 'stranded' in their respective stratigraphic profiles. A number of possible

explanations exist for these apparently laterally isolated lavas. These include local eruption sources, laterally restricted extent, topography including volcanic deposits, tectonic faulting and/or folding and drainage system control, (e.g. Fig. 9).

The distribution of the separate Enni Formation geochemical groups varies substantially within the study area. Low-Ti lavas dominate the compiled stratigraphic profiles in the NE islands area (profiles 1 & 2, Fig. 8) but also comprise a relatively coherent group of similar thickness across the central islands and Sandoy. The majority of the Transitional lava flows are found in the NE islands section along with one of only two spatial occurrences of contaminated lava flows near the base. Tracking the Low-Ti lava flows laterally, there is a Low-Ti dominated section in both the central islands and Sandoy sections within the interval c. 100-400m above the Argir Beds. There is no evidence to suggest that this sequence does not form a laterally continuous extension of the main Low-Ti sequences found to the NE and so a continuous flow field is inferred. Within this main band of Low-Ti lava flows only three flows of different composition are inter-digitated with the sequence, including two High-Ti1 and one High-Ti3 lava flows. These samples provide evidence for continued eruption of these magmas during this period dominated by Low-Ti eruptions. A second occurrence of contaminated Low-Ti lava flows occurs within this main Low-Ti interval at the base of the Nólsoy profile. Outside of this main sequence of Low-Ti lava flows, two further Low-Ti samples occur away from the NE islands section. The first sits directly above the Argir Beds at Fossdalur, and may correlate back to the main NE profiles. The second occurs isolated within the Sandoy profile. No Low-Ti lava flows are observed in the upper half of both the central islands and Sandoy profiles suggesting that these lava flows were displaced by the build-up of a more proximally erupted High-Ti flow field within this area at this time.

High-Ti1 lava flows are generally dominant in the basal parts of the central islands and Sandoy sample profiles but are also sporadically present in the NE islands section

forming the only high $TiO_2$ representatives in that profile. In the NE Viðoy profile two High-Ti1 lavas are found either side of Transitional group lava flows below the Argir Beds surface and then a single isolated flow is also found near the top of the same section. The lower two lava flows may potentially be traced back to the larger package of High-Ti1 lava flows that dominate the Fossdalur section below the Argir Beds surface, however, the upper flow must again represent a laterally discontinuous flow that does not reach the profile slightly further to the SE. In the basal parts of the central islands and Sandoy sections, High-Ti1 lava flows become inter-digitated with Low-Ti and High-Ti2 flows prior to the last High-Ti1 flow at c. 200 m above the Argir Beds.

Each compositional group dominates the eruptive sequence for short periods with the flow group thickness variations between the profiles suggesting that the High-Ti1 and High-Ti2 lava flows became progressively focused towards the south, whilst the Low-Ti lava flows in contrast became dominant in the north. The distribution data for the High-Ti1 and High-Ti2 lava flows clearly indicates that they were being erupted coeval to the Low-Ti lava flows, but were more prevalent in the south. In contrast, they largely preceded the eruption of High-Ti3 lava flows and entirely preceded the eruption of High-Ti4 flows. Based on the current group subdivision parameters, High-Ti2 lava flows largely post-date High-Ti1 lava flows, however, some overlap existed between the two groups. Spatially, High-Ti2 flows appear to have been restricted to the central islands and Sandoy areas whereas High-Ti1 lava flows reached all parts of the study area albeit in lesser quantities to the north.

High-Ti4 lava flows comprise the most spatially restricted group of the Enni Formation. The group dominates the interval c. 415-540 m above the Argir Beds on Sandoy within which no other lava groups are present. The only exception is a solitary High-Ti4 lava flow that is observed in the study area occurring at c. 300 m in the Nólsoy Profile. The surrounding lava flows and correlation panel make the joining of this sample to the main

Sandoy group relatively straightforward and so it appears that the High-Ti4 lava flows were erupted during a distinct temporally and spatially constrained interval in the southern area of the Faroe Islands.

High-Ti3 lava flows also define a spatially and stratigraphically well constrained interval. Aside from a single isolated lava flow found in the Sandoy profile below a package of Low-Ti and High-Ti1 lava flows, High-Ti3 flows dominate the final stages of the Enni Formation eruptions in the central islands and Sandoy localities. The base of the High-Ti3 lava flows in the Sandoy profile is ~240 m higher than the base of the sequence in the central islands, relative to the Argir Beds. This may be explained, in part, by the much thicker sequence of High-Ti4 lava flows present on Sandoy compared to the central islands section, c.100 m difference, potentially representing a constructional edifice focused towards the south. This still leaves c.140 m difference between the two sections. Interestingly, the tie lines for all proposed chemical correlations between the central islands and Sandoy display a progressive increase from c. 60 m to c. 120 m to c. 240 m difference with increasing stratigraphic height. This could imply that the proposed offset for the Skopunarfjørður fault, c. 200-300 m down-faulting to the south between Nólsoy and Sandoy (Passey, 2009; Passey & Varming, 2010), may be larger than predicted. The progressive increase in offset could also be the result of syn-eruptive faulting or alternatively reflect variations in eruption sites during this time, in line with the proposed development of competing shallow shield volcanoes during this time as suggested by Jolley & Passey (2013).

All of the Transitional lava flows are found in close association to Low-Ti lava flows aside from one sample in the Nólsoy profile which occurs c. 100 m above the last Low-Ti sample, postdating three significant interbeds and three separate High-Ti lava packages. In all but two instances, these Transitional lava flows are also found within c. 60 m of High-Ti lava flows. These stratigraphic associations appear consistent with subsurface mixing.

In the study area, weak crustal contamination signatures are only found in association with the Low-Ti lava flows. These occur in two distinct locations within the stratigraphy, below the Argir Beds in the NE islands profile (-150 m to -230 m) and also towards the base of the Nólsoy profile in the central islands area (130 m to 170 m). Both occurrences are found associated with interbeds of variable thickness supporting evidence for eruption hiatuses at these times and therefore, extended magma chamber storage times potentially enabling greater crustal assimilation.

In summary, the distribution patterns for the geochemically defined lava groups of the Enni Formation show a number of coherent spatial and temporal variations. As already reported in the literature (Waagstein, 1988; Passey & Jolley, 2009; Søager & Holm, 2011), the MORB-like Low $TiO_2$ lava flows are dominant in the NE of the islands, but have also been found to form a continuous interval of lava flows throughout the entire FIBG study area. This sequence decreases in thickness from the NE to the central islands section, but remains essentially constant from there to the furthest south Sandoy profile. Minor inter-digitation between these Low-Ti lava flows and all but the High-Ti4 flows is observed over this interval. High-Ti lava groups are also present over the entire study area, but are volumetrically dominant towards the south. The distribution of High-Ti4 appears to be very localized and sourced to the south based on the available data. The top of the FIBG is dominated by Low-Ti lava flows in the NE and by High-Ti3 lavas in the central islands and Sandoy sections. From the current data, it is clear that the High-Ti3 lavas on Sandoy are stratigraphically higher than those of the Low-Ti lavas in the NE. The fact that the islands have undergone differential erosion means that it cannot be excluded that the Low-Ti lava flows may have been deposited in the NE at an equivalent time to those of the High-Ti3 lava flows in the south, however, based on the current study, High-Ti3 lava flows are the uppermost, and potentially youngest exposed remnants of the FIBG.

**Discussion**

The Malinstindur and Enni formations have been correlated, based on basalt geochemistry, with the Milne Land Formation (Larsen *et al.,* 1999) and subsequently the Geikie Plateau and Rømer Fjord Formations (Søager & Holm, 2009) of Central East Greenland. Isotopic studies by Søager & Holm (2009; 2011) identified that the main High-Ti and Low Ti groups found on the Faroe Islands comprise separate mantle sources, which they suggest are associated with zoned regions of both enriched and depleted material within a proto-Icelandic plume. The Malinstindur and Enni formations are thought to have been erupted rapidly in as little as 300,000 years (Passey & Jolley 2009), equivalent to the East Greenland succession above the layered Skaergaard intrusion (Larsen & Tegner, 2006). Important to the accuracy of these correlations, and to testing the correlative potential of lava flow geochemistry in general, are detailed investigations into the spatial and temporal evolution of lava chemical types. Within this study, the sample coverage within the final stages of the FIBG has been significantly extended. By integration of the new data with the published chemical divisions of Søager & Holm (2009; 2011), mapping of the separate sources, based on incompatible trace element systematics, has enabled the spatial and relative temporal distribution of these lava groups to be investigated across the Faroe Islands.

A temporal progression from High-Ti1 to High-Ti2 to High-Ti3 lava types was identified from the sampling of Søager & Holm (2009) and used to infer a stratigraphic evolution similar to that of the Milne Land to Geikie Plateau to Rømer Fjord Formations of Central East Greenland (Larsen et al., 1989). In the current study, it is clearly identified that the High-Ti1 and High-T2 lava types are inter-digitated on the Faroe Islands. This demonstrates that these geochemical groups were erupted during overlapping time periods and, therefore, precludes their correlation at the chronostratigraphic formation level. A

similar progression in magmatic dynamics that fed the FIBG and East Greenland lava piles is not precluded, and on the contrary, appears most likely (Søager & Holm, 2009), the change was simply progressive in contrast to being temporally distinct.

The progression from High-Ti2 to High-Ti3 appears to be more stratigraphically constrained with only a single High-Ti3 lava flow being identified below the youngest package of the High-Ti2 lava flows within the Sandur section on Sandoy. This single flow may represent a short-lived precursor to the main eruption phase of the High-Ti3 lava flows.

The distribution of the lava types on the Faroe Islands reveals a complex spatial and temporal stratigraphic evolution where any single stratigraphic profile within the c. 60 km extent will give a variably incomplete history if treated as a generalized chronostratigraphic chemical section. Given these constraints, the general progression from larger (High-Ti1 and High-Ti2) to smaller (High-Ti3 and High-Ti4) melt fractions identified from Central East Greenland and the Faroe Islands (Tegner et al. 1998; Søager & Holm 2009) appears to be broadly robust for the latter stages of the High-Ti Enni Formation groups. The key constraint identified from the current study is that the progression was not linear and the derived flow fields overlapped in space and time.

The distribution of Low-Ti lavas within the Enni Formation of the FIBG display a number of interesting features. The data confirms the previously reported dominance of Low-Ti lava flows towards the north of the Faroe Islands. The distribution of the Low-Ti lava flows compared to the High-Ti lava flow sequences varies through time, with the front between the different compositions moving significantly across the islands during the final stages of volcanism. During one interval, c. 200-300 m above the Argir Beds, the Low-Ti lava flows formed a continuous flow field across the entire exposed remnants of the FIBG potentially with implications for Low-Ti lavas reaching beyond into the Faroe Shetland Basin at this time. Prior to and after this southward excursion, the Low-Ti flow fields appear to

have been displaced northwards by the accumulation of extensive High-Ti lava flow fields, likely representing low angle shield volcanoes which appear to have been erupted further to the south. From the evidence outlined in this study along with the data from East Greenland (Larsen et al. 1999; Søager & Holm 2009; Waight & Baker 2012), it is clear that the Low-Ti and High-Ti lava flows were being produced and erupted simultaneously during this time. Waight & Baker (2012) and Søager & Holm (2009), both propose that the Low-Ti melts from East Greenland and the Faroe Islands respectively were derived from depleted components within the proto-Icelandic plume.

If the broad correlation of High-Ti lava types is accepted, then at least two possible scenarios for the margin magmatic development at this time may be envisaged. Firstly, it could be that near identical High-Ti melting regimes occurred symmetrically on either side of a thinned lithospheric zone of Low-Ti melt production (e.g. Figure 10a) as proposed by Søager & Holm (2009; 2011). Alternatively, a situation could be envisaged whereby the High-Ti melts were being produced within a more continuous melting region, with the Low-Ti lavas initially being fed into the High-Ti flow fields from an area of progressively thinning lithosphere to the west (e.g. Fig. 10b). A non-uniform rifting and thinning scenario could have been enhanced by the presence of a major transform zone between the Faroe Islands and the Blosseville Kyst region of East Greenland (e.g. Guarnieri, 2015). Such a feature could, therefore, have promoted earlier thinning of the lithosphere to the west and east of the Faroe Islands in the lead up to and early onset of rifting.

In such a setting, longer melt columns producing the first locally sourced Low-Ti melts would have been initially restricted to the west and east of the Faroe Islands. At the same time, a semi-continuous region of High-Ti melt production, requiring relatively thicker lithosphere, could have existed across the fault zone between the FIBG and the Blosseville Kyst for longer, explaining the close similarities between the FIBG and East Greenland

successions without requiring independently near symmetrical melting regimes on either side of a continuous zone of Low-Ti melting.

The proposed site of the proto-Icelandic anomaly under either central (Lawver & Müller, 1994), or central east (Torsvik et al., 2015) Greenland at the time, could also potentially raise questions as to the presence of symmetrical melt columns on either side of the rift system. Upwelling mantle material convecting along the base of the lithosphere from the anomaly source (e.g. Hartley et al., 2011), would have reached East Greenland first, but would then have had to pass through a High-Ti followed by Low-Ti melting regime prior to reaching the Faroe Islands, which does not appear to be supported by the isotopic evidence which suggests separate mantle sources for the Low and High-Ti samples (Søager & Holm, 2009; 2011). We therefore tentatively suggest that the melting regions for the Low and High-Ti suites were controlled by non-uniform thinning along the rift axis during the Late Palaeocene to Early Eocene. The lateral and vertical juxtaposition of the lava suites on both the Faroe Islands and East Greenland were fed by magmas sourced in separate melting regions which fed magmas in some cases potentially tens to hundreds of km laterally, either through the lithosphere, across the surface, or both, away from their original melting regions. Significant lateral migration of magma within volcanic rifted margin settings is becoming widely recognised within the literature, (e.g. Schofield et al., 2015; Magee et al., 2016), supporting a greater role for lateral migration and inter-digitation of associated magma geochemical signatures (e.g. Hole et al., 2015).

No clear correspondence between flow facies type and chemical groups has been observed within the Enni Formation sample profiles. This suggests that the separate magma-suites did not impart a diagnostic or differentiable set of eruption dynamics onto the resulting lava flows, unlike for example in the cases of the older Malinstindur (compound braided lava dominated) and Beinisvørð (simple tabular lava dominated) Formations of the FIBG. The

resulting variations in the areal distribution of the separate lava flow facies within the Enni Formation, has imparted a strong facies control on the correlation potential of the separate magma types across the islands.

These results have implications for the potential of lava chemistry as a tool for stratigraphic correlation within extrusive lava flow sequences, along with questioning the likely representativeness of individual vertical or composite profiles in similar settings. In many settings worldwide, correlation within extrusive lava flow packages in the sub-surface of LIPs forms an important requirement for resource management as for example in the case of both inter-lava (e.g. Schofield & Jolley, 2013; Ebinghaus et al., 2014) and intra-lava (Burns et al., 2012) hosted reservoirs. Geophysical logging data from boreholes penetrating volcanic intervals may in some cases provide useful information for attempting inter-well correlation based for example on gamma log variations which record the U, Th and K contents of separate flow packages and soil horizons (e.g. Buckley & Oliver, 1993; Helm-Clark et al., 2004). However, in many other cases, the uniformly low primary gamma response of thick lava packages (e.g. Planke, 1994; Nelson et al., 2009; Millett et al., 2015) may limit the viability of geophysical means for borehole correlation, outside of facies characterization (e.g. Nelson et al., 2009) which, as demonstrated by this study, does not form a robust criteria for correlation by itself. Seismic data, where available forms the most commonly used method for sub-surface correlation, however, imaging challenges relating to the heterogeneous velocity, density and structure of thick volcanic sequences commonly results in poor resolution imaging of volcanic sequences (Davison et al., 2010). Where drill cuttings of sufficiently good quality (Millett et al., 2014), core or sidewall core data are available from boreholes, the chemical composition of thick lava sequences may be revealed (e.g. Millett et al., 2015). In such cases, lava flow geochemistry opens the potential for igneous geochemistry to play an important role in subsurface correlation. In the current study,

we highlight the importance of integrating volcanic facies with chemical stratigraphy to enable correlation within basaltic LIP sequences. Our results highlight the potential but also the limitations for chemical correlation where competing magmatic plumbing systems erupt mixed facies lava flows across extensive subaerial regions. The implications of the current study stretch beyond the FIBG and the NAIP and have general implications for field or sub-surface correlations within large igneous province flow fields in general.

**Conclusions**

By systematic stratigraphic sampling of the youngest preserved lava sequences of the Enni Formation, this study has investigated the temporal and spatial development of magmatism during the syn-rift volcanism. From this study the following conclusions may be drawn:

1. Based on major and trace element systematics, one Low-Ti and four High-Ti lava groups are identified which cannot be related by simple upper crustal magmatic processes such as fractionation, contamination or crystal accumulation.

2. Integration of sample profiles into a high resolution 3D ArcGIS model for the Faroe Islands, including the regionally extensive Argir Beds marker unit, has enabled detailed stratigraphic comparisons between the separate islands.

3. Low-Ti lava flows dominate in the north of the islands, but at times formed a continuous flow field across the islands stretching south beyond the current FIBG exposures towards the Faroe-Shetland Basin.

4. High-Ti lava flows dominate the central and southern Enni Formation and display a general progression from larger (High-Ti1 and High-Ti2) to smaller (High-Ti3 and High-Ti4) melt fractions consistent with the general progression identified from East Greenland.

5. Overlap in the progression of the lava flows from the four High-Ti groups suggests that they are not chronostratigraphically constrained and, therefore cannot be directly used as formation equivalents to East Greenland, albeit that the dominant progression appears broadly equivalent.

6. Correlation is restricted to the local (10's km scale) within the Enni Formation as a consequence of the number of chemically distinct magmatic systems and their mixed compound/tabular lava flow facies.

7. The incursion of Low-Ti lava flows across the Faroe Islands accompanied the onset of significant lithospheric thinning and was also contemporaneous with High Ti lava flows produced beneath thicker lithosphere on the rift flanks of the Faroe Islands and East Greenland.

8. The Low-Ti lava flows may have separated near identical High-Ti melt columns on either side of the rift, or alternatively, could have been fed across a broader area of still relatively thick lithosphere associated with a strike-slip zone between the FIBG and Blosseville Kyst region of East Greenland.

**Figure Captions**

**Figure 1.** *a. Location map showing the position of the Faroe Islands within the North Atlantic Igneous Province (modified after Larsen et al. 1999), BPIP; British Palaeogene Igneous Province. b. Geological map of the Faroe Islands Basalt Group (FIBG) showing the distribution of the main formations (after Passey & Jolley 2009) and the sample locations from this study. c. Composite stratigraphic section through the FIBG (Passey & Jolley 2009). d. Field example of the Argir Beds outcropping on Sandoy.*

**Figure 2**. *Summary facies logs for the sample profiles through the Enni Formation showing the volcanic facies type, sample locations and general petrographic properties of each sample transect relative to the Argir Beds 3D GIS surface.*

**Figure 3**. *a. Sample transect showing the location of the Argir Beds and hillside flow morphology examples from the sample transect up the Enni mountain on Viðoy, NE Faroe Islands. Solid lines represent sampling profiles, dashed line represents the tie-line between the two sample profiles. b. Cliff side examples of mixed simple (S) and compound (C) braided lava flow morphologies from the southern end of Svínoy. The occurrence of thin reddened volcaniclastic sedimentary units is significantly clearer in cliff sections compared to the weathered hillside section. c. Detail of the clear colour variations between differing compositions of lavas (in this example brown-weathering: Low-Ti; pale weathering: High-Ti1) exposed in the upper section of the sample profile on Viðoy (Fig. 3.a). d. Annotated close-up examples of compound and simple lava flow facies from Svínoy (Fig. 3.b).*

**Figure 4**. *Selected major and trace element plots for the Enni Formation. a. Mobile elements Sr ppm and $K_2O$ wt.% versus incompatible Zr ppm for different LOI wt.% ranges. b. $Al_2O_3$ wt.% versus MgO wt. % with vectors showing the effect of $An_{70}$ plagioclase addition. c. $P_2O_5$ wt.% versus Zr ppm displays a strong linear regression intersecting the origin. d. Ba/Zr versus $SiO_2$ wt.% with the range of data from variably crustally contaminated ODP Leg 152 basalts plotted for comparison (Larsen et al., 1998). All presented major element data has been recalculated to 100 wt. % on a dry basis with a fixed oxidation ratio of $Fe_2O_3/FeO = 0.15$.*

**Figure 5.** *Selected major elements (wt. %) plotted versus Mg# (100\* atomic $Mg^{2+}/ (Mg^{2+}+Fe^{2+})$). Petrolog3 (Danyushevsky, 2001) liquid line-of-descent forward models for crystallization of Enni low $TiO_2$ primary magma for sample GL-1-11 at variable pressures are shown for CaO vs. Mg#. Details of the calculation of primary magma to sample GL-1-11 are given in Hole & Millett, (2016). The primary magma was formed at a mantle potential temperature $T_P = 1551°C$ and represents an accumulated melt fraction of 0.27. The initial pressure of the intersection of the dry peridotite solidus was 4.5 GPa and the final pressure*

*of melting was 2.8 GPa. Petrolog3 model parameters; olivine – melt $K_D$, Beattie (1993); plagioclase – melt $K_D$ and clinopyroxene – melt $K_D$, Danyuchevsky (2001); QFM buffer, Borisov & Shapkin (1990). All presented major element data has been recalculated to 100 wt. % on a dry basis with a fixed oxidation ratio of $Fe_2O_3/FeO = 0.15$.*

**Figure 6.** *Nb and Y versus Zr along with Y versus Nb and Nb/Y versus V for the Enni Formation lava flows. Lines display constant inter-element ratios intersecting the origin for separate groups. Data fields from Søager & Holm (2009 & 2011) are presented for comparison.*

**Figure 7.** a. *REE multi-element plot showing representative samples from the main chemical groups, all elements normalized to primitive mantle (PM) after McDonough & Sun (1995). b. PM normalised $Dy/Yb_n$ versus $La/Yb_n$ for the Enni Formation groups. Curves show non-modal incremental batch melting of a slightly depleted PM source, from a nominal starting composition of 75% PM (McDonough & Sun (1995) + 25% DMM (Workman & Hart 2005). 2% melt was retained within the residue after each 1% melting increment. Initial mineral modes for PM and DMM are from Fram & Lesher (1993) and Workman & Hart (2005) respectively. Partition coefficients for olivine (ol), clinopyroxene (cpx), orthopyroxene (opx) and garnet (gt) are from Halliday et al. (1995) and those for spinel (sp) are from McKenzie & O'Nions (1991). Arbitrary mixing lines between the garnet+spinel and spinel field melts are plotted to demonstrate the potential contributions from separate depth regions. The non-modal batch melting models and mixing lines derived by Waight & Baker (2012) for East Greenland Low-Ti melts are presented in pale blue as a closer representation for the MORB-like Low-Ti lava flows. Crosses display 1% increments on the melting lines and 10% increments on the mixing lines. Inset displays extension of same plot.*

**Figure 8.** *Geochemical stratigraphic correlation panel for the late stage FIBG development. Breaks in the solid colour bars next to each stratigraphic section represent intervals where the samples comprise high LOI, high $Al_2O_3$, are undefined or where exposure gaps were*

*encountered. Where high LOI and Al2O3 samples fit into one of the main groups, this is noted within the supplementary data. The correlation tie lines therefore represent a minimum complexity scenario in each case.*

**Figure 9.** *Schematic representation of selected flow field features which may restrict the lateral continuity of lava flows or flow groups.*

**Figure 10.** *Simplified conceptual cross sections highlighting possible variations in melt production localization between East Greenland and the Faroe Islands during the syn-rift phase development. A. Scenario displaying a region of Low-Ti melt generation beneath thinned lithosphere separating two near-symmetrical regions of High-Ti melting. Inset map showing continuous zone of Low-Ti melt production between the Faroe Islands and East Greenland (base map after Jolley & Morton, 2007). B. Non-uniform thinning scenario whereby thinning is focused to the west of the Faroe Islands during early rifting, allowing a near-continuous zone of High-Ti melt production beneath thickened lithosphere between the Faroe Islands and East Greenland prior to full continental rupture.*

**Table 1.** *Selected XRF major and trace element data and ICP-MS REE data for examples from each of the main chemical groups. Full analyses for all samples including international reference runs are available within the online supplementary resources.*

**Table 2.** *Chemical criteria used for distinguishing the separate chemical groups within this study.*

**Acknowledgements**

**References**

Babechuk, M.G., Widdowson, M., Kamber, B.S., 2014. Quantifying chemical weathering intensity and trace element release from two contrasting basalt profiles, Deccan Traps, India. Chemical Geology 363, 56-75.

Beattie, P., 1993. Olivine-melt and orthopyroxene-melt equilibria. Contributions to Mineralogy and Petrology 115, 103–111.

Borisov, A.A., Shaplin, A.I., 1990. A new empirical equation rating Fe3+/Fe2+ in magmas to their composition, oxygen fugacity, and temperature. Geochemistry International 27, 111-116.

Bott, M.H.P., Sunderland, J., Smith, P.J., Casten, U., Saxov, S., 1974. Evidence for continental crust beneath the Faeroe Islands. Nature 248, 202–204.

Buckley, D.K., and Oliver, D., 1990. Geophysical logging of water exploration boreholes in the Deccan Traps, Central India. Geological Society, London, Special Publications, 48(1), 153-161.

Burns, E.R., Snyder, D.T., Haynes, J. V., Waibel, M.S., 2012. Groundwater Status and 739 Trends for the Columbia Plateau Regional Aquifer System, Washington, Oregon, and 740 Idaho. U.S. Geological Survey Scientific Investigations Report 2012-5261.

Casten, U., 1973. The crust beneath the Faeroe Islands. Nature Physical Science 241, 83–4.

Danyushevsky, L.V., 2001. The effect of small amounts of $H_2O$ on crystallisation of mid-ocean ridge and backarc basin magmas. Journal of Volcanology and Geothermal Research 110, 265–280.

Davison, I., Stasiuk, S., Nuttall, P., Keane, P., 2010. Sub-basalt hydrocarbon prospectivity in the Rockall, Faroe–Shetland and Møre basins, NE Atlantic. Geological Society London, Petroleum Geology Conference series 7, 1025-1032.

Debaille, V., Blichert-Toft, J., Agranier, A., Doucelance, R., Schiano, P., Albarède, F., 2006. Geochemical component relationships in MORB from the Mid-Atlantic Ridge, 22–35°N. Earth and Planetary Science Letters 241, 844–862.

Ebinghaus, A., Hartley, A.J., Jolley, D.W., Hole, M., and Millett, J., 2014. Lava–sediment interaction and drainage-system development in a large igneous province: Columbia River Flood Basalt Province, Washington State, USA. Journal of Sedimentary Research 84(11), 1041-1063.

Fitton, J.G., Saunders, A.D., Larsen, H.C., Hardarson, B.S., Norry, M.J., 1998. Volcanic rocks from the East Greenland margin at 63°N: composition, petrogenesis and mantle sources. In: Saunders, A.D., Larsen, H.C., Wise, S., Allen, J.R., (eds) Proceedings of the Ocean Drilling Program, Scientific Results, 152. Ocean Drilling Program, College Station, TX, 331–350.

Fram, M.S., Lesher, C.E., 1993. Geochemical constraints on mantle melting during creation of the North Atlantic basin. Nature 363, 712–715.

Fridleifsson, G.O., Elders, W.A., 2005. The Iceland Deep Drilling Project: a search for deep unconventional geothermal resources. Geothermics 34, 269–285.

Gariépy, C., Ludden, J., Brooks, C., 1983. Isotopic and trace element constraints on the genesis of the Faroe lava pile. Earth and Planetary Science Letters 63, 257–72.

Guarnieri, P., 2015. Pre-break-up palaeostress state along the East Greenland margin. Journal of the Geological Society 172(6), 727-739.

Hald, N., Waagstein, R., 1983. Silicic basalts from the Faeroe Islands: evidence of crustal contamination. In: Bott, M. H. P., Saxov, S., Talwani, M. & Thiede, J. (eds) Structure and Development of the Greenland–Scotland Ridge. New Methods and Concepts. New York, Plenum Press, 343–349.

Halliday, A.N., Lee, D., Tommasini, S., Davies, G.R., Paslick, C.R., Fitton, J.G., James, D.E., 1995. Incompatible trace elements in OIB and MORB and source enrichment in the sub-oceanic mantle. Earth and Planetary Science Letters 133, 379–395.

Hartley, R.A., Roberts, G.G., White, N., Richardson, C., 2011. Transient convective uplift of an ancient buried landscape. Nature Geoscience 4(8), 562-565.

Helm-Clark, C.M., Rodgers, D.W., Smith, R.P., 2004. Borehole geophysical techniques to define stratigraphy, alteration and aquifers in basalt. Journal of Applied Geophysics 55(1), 3-38.

Hole, M.J., Millett, J.M., 2016. Controls of mantle potential temperature and lithospheric thickness on magmatism in the North Atlantic Igneous Province. Journal of Petrology 57(2), 417-436.

Hole, M.J., Millett, J.M., Rogers, N.W., Jolley, D.W., 2015. Rifting and mafic magmatism in the Hebridean basins. Journal of the Geological Society 172(2), 218-236.

Holm, P.M., Hald, N., Waagstein, R., 2001. Geochemical and Pb–Sr–Nd isotopic evidence for separate hot depleted and Iceland plume mantle sources for the Paleogene basalts of the Faroe Islands. Chemical Geology 178, 95–125.

Irvine, T.N., Baragar, W.R.A., 1971. A guide to the chemical classification of the common volcanic rocks. Canadian Journal of Earth Sciences 8, 523–548.

Jerram, D.A., 2015. Hot Rocks and Oil: Are Volcanic Margins the New Frontier? Elsevier R&D Solutions.

Jerram, D.A., 2002. Volcanology and facies architecture of flood basalts. In: Menzies, M.A., Klemperer, S.L., Ebinger, C.J., Baker, J., (eds.) Volcanic Rifted Margins. Geological Society of America, Special Paper 362, 119–132.

Jolley, D.W., Bell, B.R., 2002. The evolution of the North Atlantic Igneous Province and the opening of the NE Atlantic rift. In: Jolley, D. W., Bell, B. R., (eds) The North Atlantic

Igneous Province: Stratigraphy, Tectonic, Volcanic and Magmatic Processes. Geological Society, London, Special Publications 197, 1–13.

Jolley, D.W., Passey, S.R., 2013. Lava-Sediment Interaction in a Near-Shore Environment: An Analogue for Offshore Exploration. SINDRI Report: C46-38-01, 73-94. Release date: January 2018.

Jolley, D.W., Morton, A.C., 2007. Understanding basin sedimentary provenance: evidence from allied phytogeographic and heavy mineral analysis of the Palaeocene of the NE Atlantic. Journal of the Geological Society 164(3), 553-563.

Jolley, D.W., Clarke, B., Kelley, S., 2002. Paleogene time scale miscalibration: evidence from the dating of the North Atlantic igneous province. Geology 30, 7–10.

Jolley, D.W., Passey, S.R., Hole, M.J., Millett, J.M., 2012. Large-scale magmatic pulses drive plant ecosystem dynamics. Journal of the Geological Society, London 169(6), 703–711.

Jørgensen, O., 1984. Zeolite zones in the basaltic lavas of the Faeroe Islands. A quantitive description of the secondary minerals in the deep wells of Vestmanna-1 and Lopra-1. In: Berthelsen, O., Noe-Nygaard, A., Rasmussen, J., (eds) The Deep Drilling Project 1980–1981 in the Faeroe Islands, Annales Societatis Scientiarum, Færoensis, Supplementum, IX, 71–92.

Jørgensen, O., 2006. The regional distribution of zeolites in the basalts of the Faroe Islands and the significance of zeolites as palaeotemperature indicators. In Chalmers, J.A. & Waagstein, R. (eds) Scientific Results from the Deepened Lopra-1 Borehole, Faroe Islands. Geological Survey of Denmark and Greenland Bulletin 9, 123–56.

Kent, A.J.R., Baker, J.A., Wiedenbeck, M., 2002. Contamination and melt aggregation processes in continental flood basalts: constraints from melt inclusions in Oligocene basalts from Yemen. Earth and Planetary Science Letters 202, 577-594.

Kerr, A.C., 1995. The geochemical stratigraphy, field relations and temporal variation of the Mull–Morvern Tertiary lava succession. Transactions of the Royal Society of Edinburgh, Earth Sciences 86, 35–47.

Larsen, L.M., Fitton, J.G., Fram, M.S., 1998. Volcanic rocks of the Southeast Greenland margin in comparison with other parts of the North Atlantic Tertiary Igneous Province. In: Saunders, A.D., Larsen, H.C., Wise, S.W.J., (eds) Proceedings of the Ocean Drilling Program, Scientific Results, 152. Ocean Drilling Program, College Station, TX, 315–330.

Larsen, L.M., Waagstein, R., Pedersen, A.K., Storey, M., 1999. Trans-Atlantic correlation of the Palaeogene volcanic successions in the Faeroe Islands and East Greenland. Journal of the Geological Society, London 156, 1081–1095.

Larsen, L.M., Watt, W.S., Watt, M., 1989. Geology and petrology of the Lower Tertiary plateau basalts of the Scoresby Sund region, East Greenland. Geology of Greenland Survey Bulletin 157, 1–164.

Larsen, R. B., Tegner, C., 2006. Pressure conditions for the solidification of the Skaergaard intrusion: Eruption of East Greenland flood basalts in less than 300,000 years. Lithos 92, 181–97.

Lawver, L.A., Müller, R.D., 1994. Iceland Hotspot Track. Geology 22, 311-314.

Le Maitre. R.W., Bateman, P., Dudek, A., Keller, J., Lameyre, J., Le Bas, M.J., Sabine, P.A., Schmid, R., Sorensen, H., Streckeisen, A., Woolley, A.R., Zanettin, B., 1989. A Classification of Igneous Rocks and Glossary of terms: Recommendations of the International Union of Geological Sciences Subcommission on the Systematics of Igneous Rocks. Blackwell Scientific Publications, Oxford, U.K.

Lundin, E.R., Doré, A.G., 2005. The fixity of the Iceland "hotspot" on the Mid-Atlantic Ridge: Observational evidence, mechanisms, and implications for Atlantic volcanic

margins, In: Foulger, G.R., Natland, J.H., Presnall, D.C., and Anderson, D.L., eds., Plates, plumes, and paradigms: Geological Society of America Special Paper 388, 627–651.

Magee, C., Muirhead, J.D., Karvelas, A., Holford, S.P., Jackson, C.A., Bastow, I.D., Schofield, N., Stevenson, C.T., McLean, C., McCarthy, W., Shtukert, O., 2016. Lateral magma flow in mafic sill complexes. Geosphere 12(3), pp.809-841.

McDonough, W.F., Sun, S. -s., 1995. The composition of the Earth. Chemical geology 120, 223–253.

McKenzie, D., O'Nions, R.K., 1991. Partial Melt Distributions from Inversion of Rare Earth Element Concentrations. Journal of Petrology 32, 1021–1091.

Millett, J.M., 2014. Unpublished PhD thesis. University of Aberdeen.

Millett, J.M., Hole, M.J., Jolley, D.W., Schofield, N., Campbell, E., 2015. Frontier exploration and the North Atlantic Igneous Province: new insights from a 2.6 km offshore volcanic sequence in the NE Faroe–Shetland Basin. Journal of the Geological Society 173(2), 320-336.

Millett, J.M., Hole, M.J., Jolley, D.W., 2014. A fresh approach to ditch cutting analysis as an aid to exploration in areas affected by large igneous province (LIP) volcanism. Geological Society, London, Special Publications 397, 193–207.

Morrison, M.A., 1978. The use of 'immobile' trace elements to distinguish the palaeotectonic affinities of metabasalts: applications to the Palaeocene basalts of Mull and Skye, NW Scotland. Earth and Planetary Science Letters 39, 407–416.

Passey, S.R., Bell, B.R., 2007. Morphologies and emplacement mechanisms of the lava flows of the Faroe Islands Basalt Group, Faroe Islands, NE Atlantic Ocean. Bulletin of Volcanology 70, 139–56.

Passey, S.R., Jolley, D.W., 2009. A revised lithostratigraphic nomenclature for the Palaeogene Faroe Islands Basalt Group, NE Atlantic Ocean. Transactions of the Royal Society of Edinburgh, Earth and Environmental Science 99, 127–158.

Passey, S.R., Varming, T., 2010. Surface interpolation within a continental flood basalt province: an example from the Palaeogene Faroe Islands Basalt Group. Journal of Structural Geology 32, 709–723.

Passey, S.R., 2009. Recognition of a faulted basalt lava flow sequence through the correlation of stratigraphic marker units, Skopunarfjørður, Faroe Islands. In Faroe Islands Exploration Conference: Proceedings of the 2nd Conference. Annales Societatis Scientiarum Færoensis, Tórshavn 50, 174-204.

Ramsey, M.H., Potts, P.J., Webb, P.C., Watkins, P., Watson, J.S., Coles, B.J., 1995. An Objective Assessment of Analytical Method Precision - Comparison of ICP-AES and xrf for the Analysis of Silicate Rocks. Chemical Geology 124 (1-2), 1-19.

Rasmussen, J., Noe-Nygaard, A., 1970 (1969). Geology of the Faeroe Islands (Pre-Quaternary) [Trans: Henderson, G.] 1/25. Copenhagen, Geological Survey of Denmark.

Reidel, S.P., Johnson, V.G., Spane, F.A., 2002. Natural Gas Storage in Basalt Aquifers of the Columbia Basin, Pacific Northwest USA: A Guide to Site Characterization. United States Department of Energy, Washington.

Richardson, K.R., White, R.S., England, R.W., Fruehn, J., 1999. Crustal structure east of the Faroe Islands: mapping sub-basalt sediments using wide angle seismic data. Petroleum Geoscience 5, 161–172.

Saunders, A.D., Fitton, J.G., Kerr, A.C., Norry, M.J., Kent, R.W., 1997. The North Atlantic Igneous Province. In: Mahoney, J.J., Coffin, M.F., (eds) Large Igneous Provinces. Geophysical Monographs, American Geophysical Union 100, 45–93.

Schofield, N., Jolley, D.W., 2013. Development of intra-basaltic lava-field drainage systems within the Faroe-Shetland Basin. Petroleum Geoscience 19, 273–288.

Schofield, N., Holford, S., Millett, J.M., Brown, D., Jolley, D.W., Passey, S., Muirhead, D., Grove, C., Magee, C., Murray, J., Hole, M., 2015. Regional magma plumbing and emplacement mechanisms of the Faroe- Shetland Sill Complex: implications for magma transport and petroleum systems within sedimentary basins. Basin Research 29, 41-63.

Søager, N.. Holm, P.M.. 2011. Changing compositions in the Iceland plume; Isotopic and elemental constraints from the Paleogene Faroe flood basalts. Chemical Geology 280, 297–313.

Søager, N., Holm, P.M., 2009. Extended correlation of the Paleogene Faroe Islands and East Greenland plateau basalts. Lithos 107 (3–4), 205–215.

Storey, M., Duncan, R.A.. Tegner, C.. 2007. Timing and duration of volcanism in the North Atlantic Igneous Province: Implications for geodynamics and links to the Iceland hotspot. Chemical Geology 241, 264-281.

Tegner, C., Lesher, C.E., Larsen, L.M., Watt, W.S., 1998. Evidence from the rare-earth-element record of mantle melting for cooling of the Tertiary Iceland plume. Nature 395, 591–594.

Torsvik, T.H., Amundsen, H.E., Trønnes, R.G., Doubrovine, P.V., Gaina, C., Kusznir, N.J., Steinberger, B., Corfu, F., Ashwal, L.D., Griffin, W.L., Werner, S.C., 2015. Continental crust beneath southeast Iceland. Proceedings of the National Academy of Sciences 112(15),.E1818-E1827.

Waagstein, R.. 1977. The Geology of the Faeroe Plateau. Unpublished PhD Thesis. University of Copenhagen.

Waagstein, R.. 1988. Structure, composition and age of the Faeroe basalt plateau. In: Morton, A.C.. Parson, L.M.. (eds) Early Tertiary Volcanism and the Opening of the NE Atlantic. Geological Society, London, Special Publications 39, 225–38.

Waagstein, R., Guise, P., Rex, D., 2002. K/Ar and 39Ar/40Ar whole-rock dating of zeolite facies metamorphosed flood basalts: the upper Paleocene basalts of the Faroe Islands, NE Atlantic. In: Jolley, D. W., Bell, B. R., (eds) The North Atlantic Igneous Province: Stratigraphy, Tectonic, Volcanic and Magmatic Processes. Geological Society, London, Special Publication 197, 219–52.

Waight, T.E., Baker, J.A., 2012. Depleted Basaltic Lavas from the Proto-Iceland Plume, Central East Greenland. Journal of Petrology 53, 1569–1596.

Watson, J.S., 1996. Fast, Simple Method of Powder Pellet Preparation for X-Ray Fluorescence Analysis. X-Ray Spectrometry 25 (4), 173-174.

Workman, R.K., Hart, S.R., 2005. Major and trace element composition of the depleted MORB mantle (DMM). Earth and Planetary Science Letters 231, 53–72.

Zakharova, N.V., Goldberg, D.S., Sullivan, E.C., Herron, M.M., Grau, J.A., 2012. Petrophysical and geochemical properties of Columbia River flood basalt: Implications for carbon sequestration. Geochemistry, Geophysics. Geosystems 13.
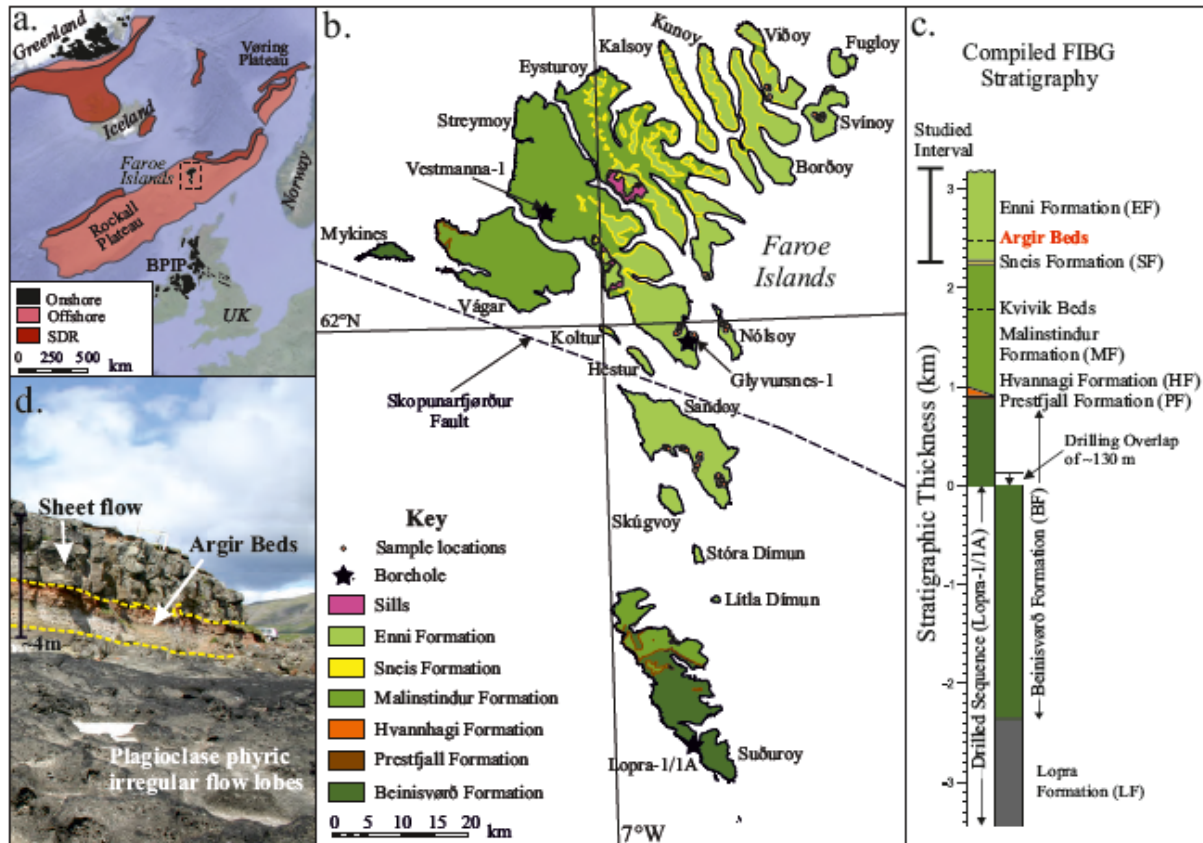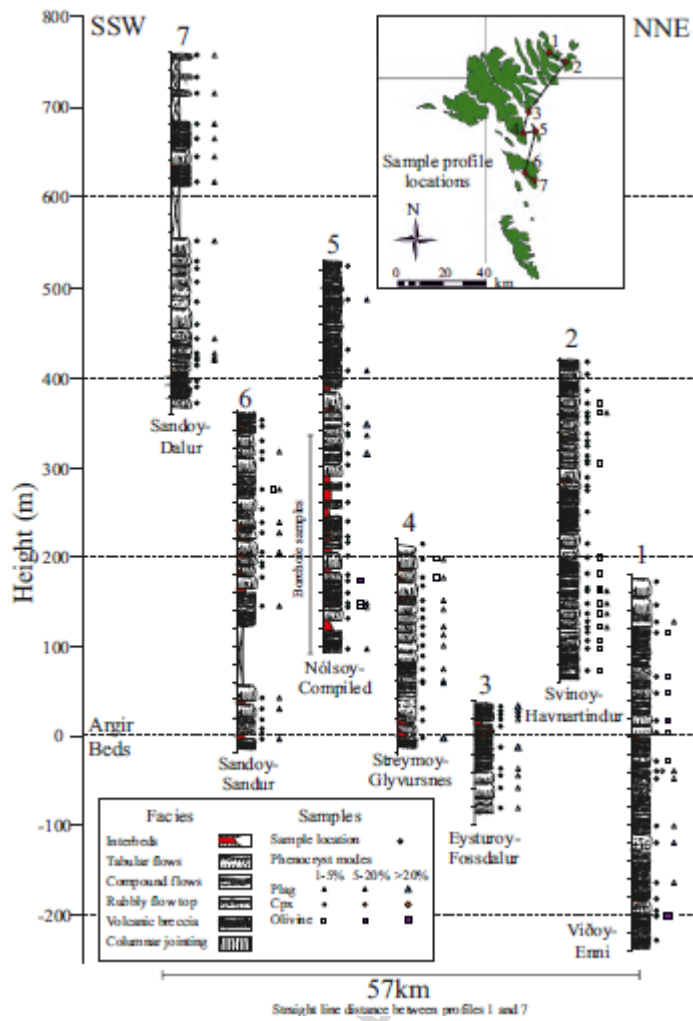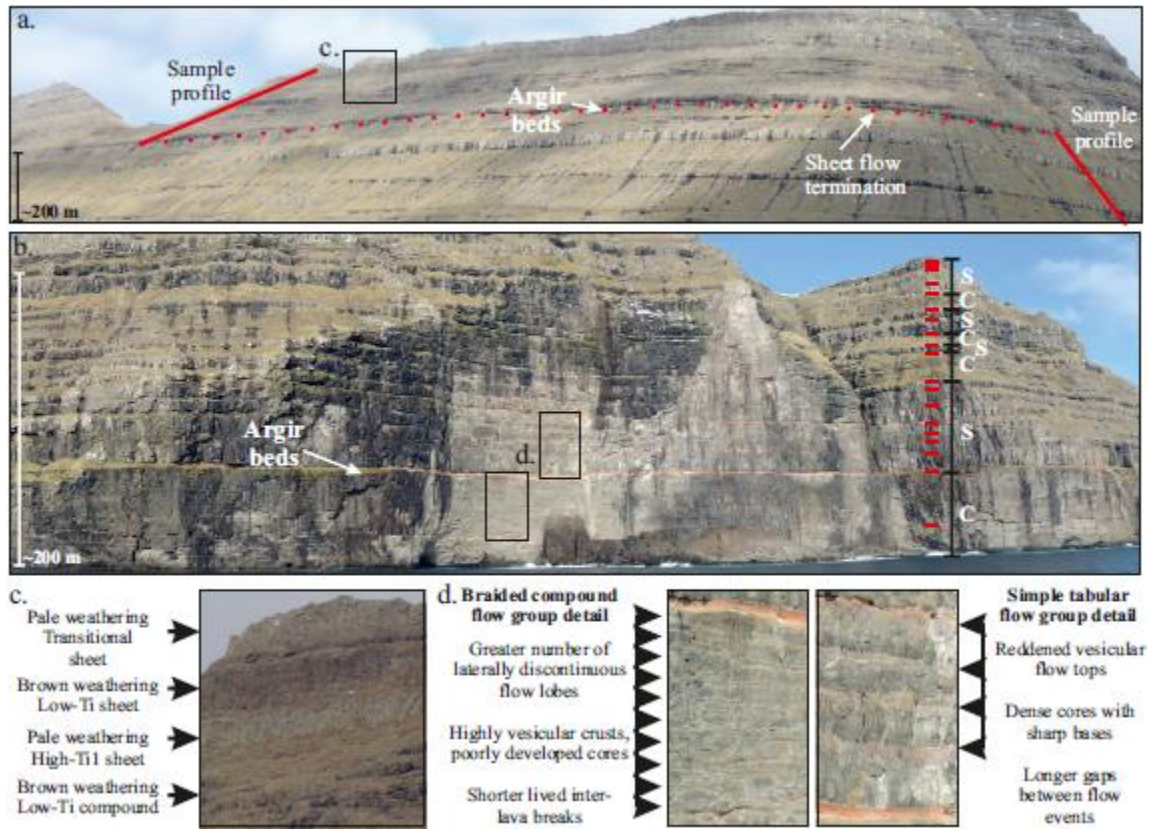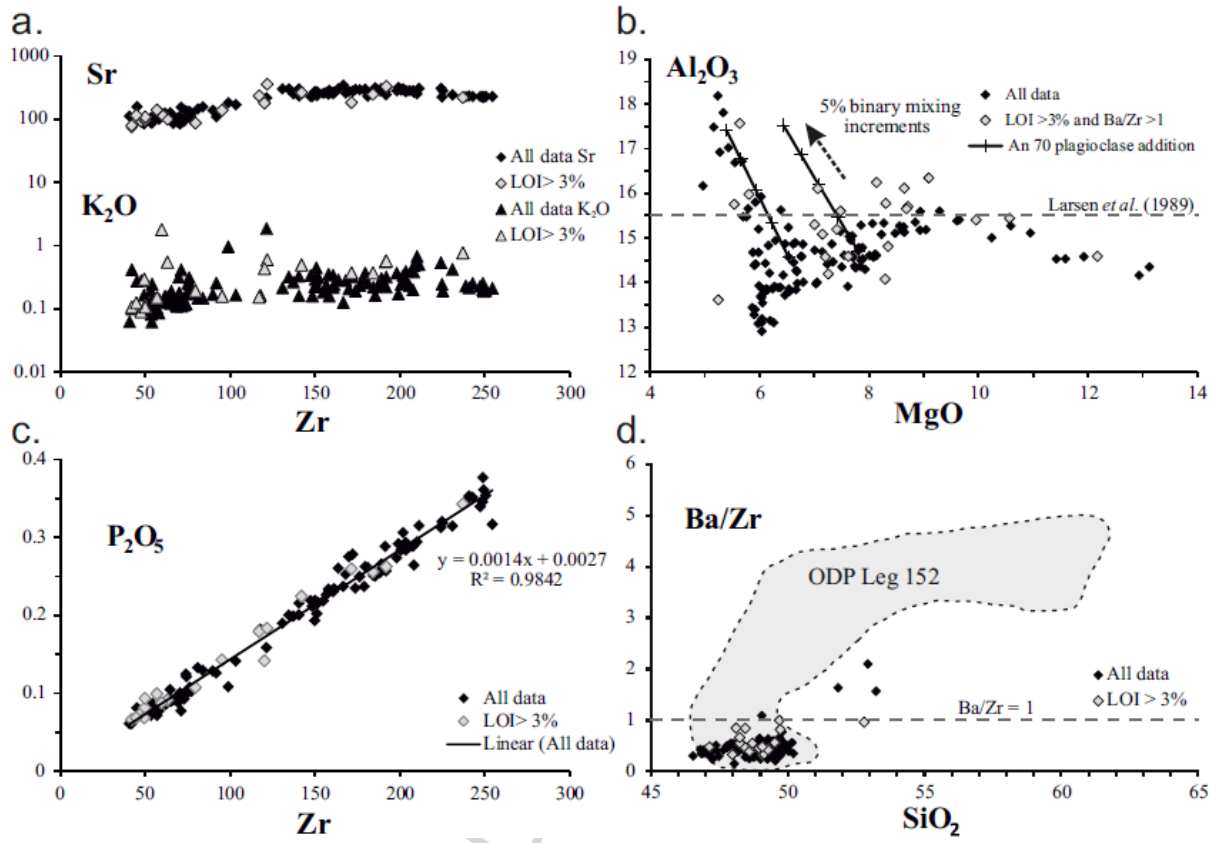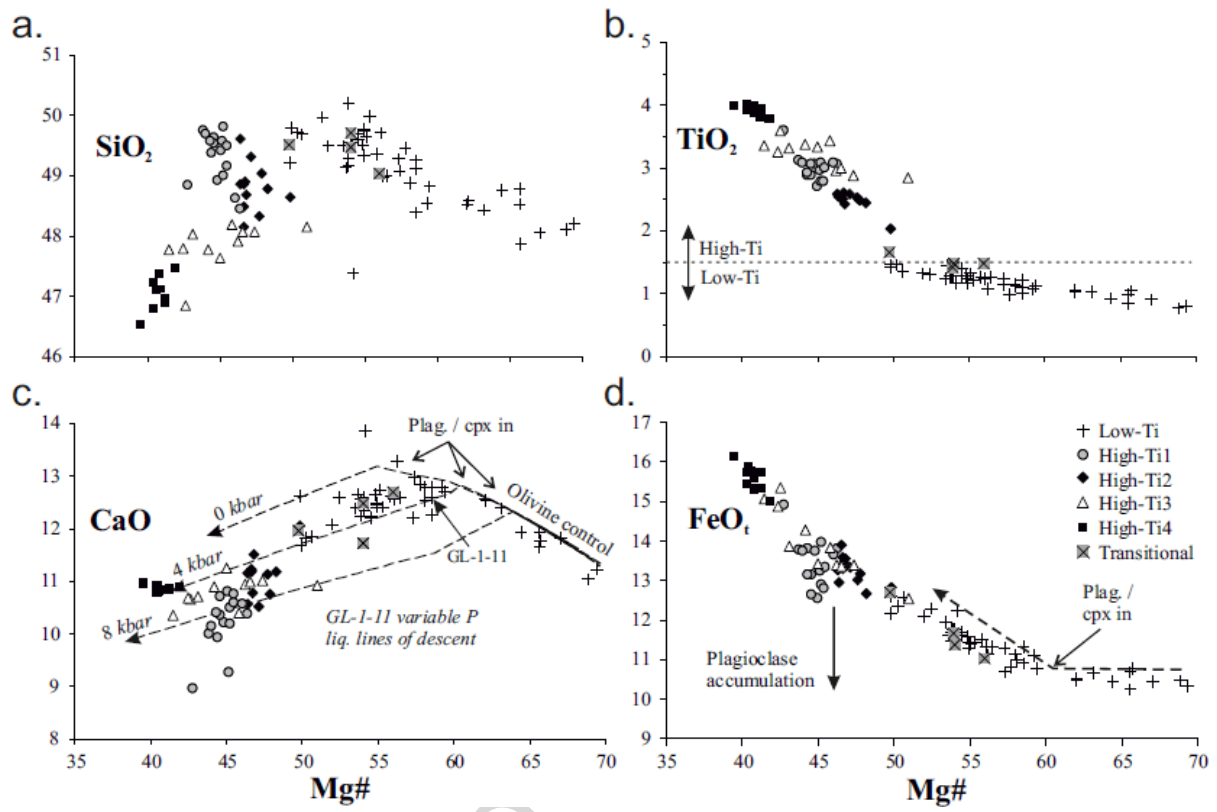
Figure 1

Figure 2

Figure 3

Figure 4

Figure 5

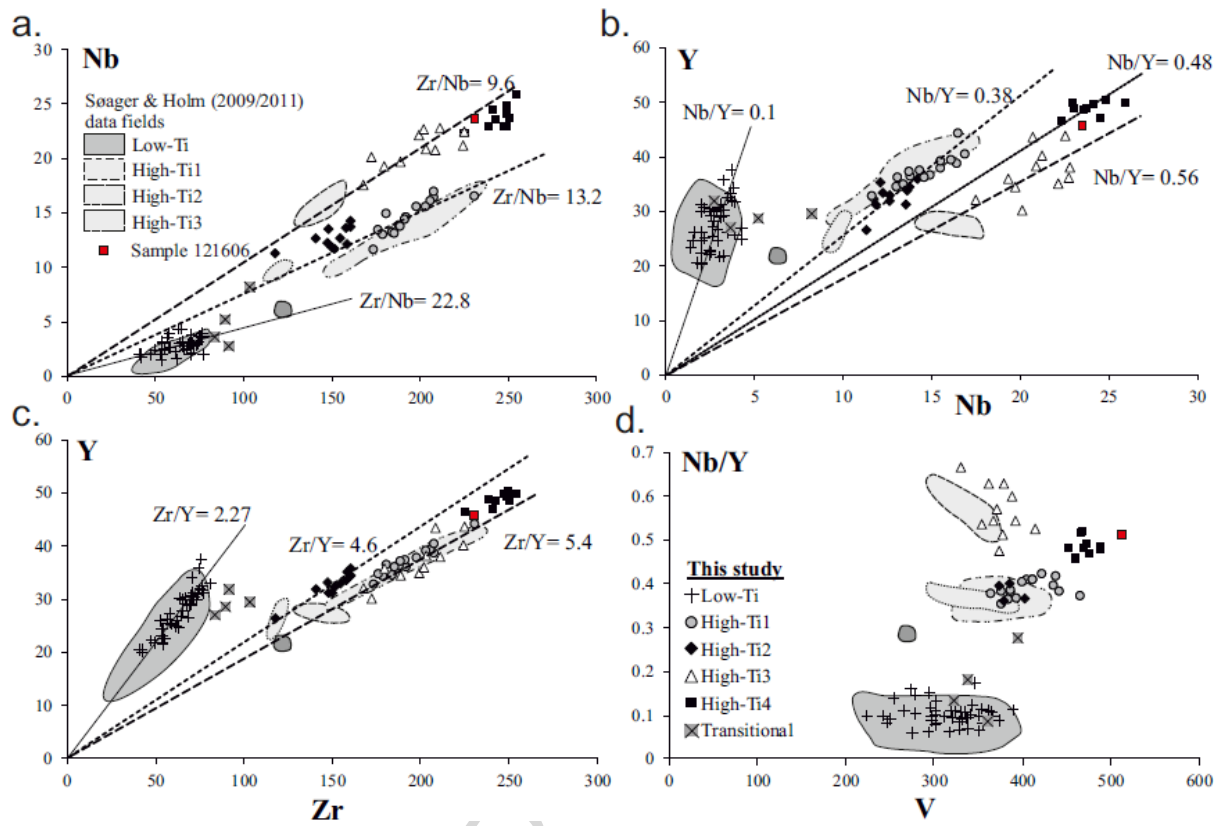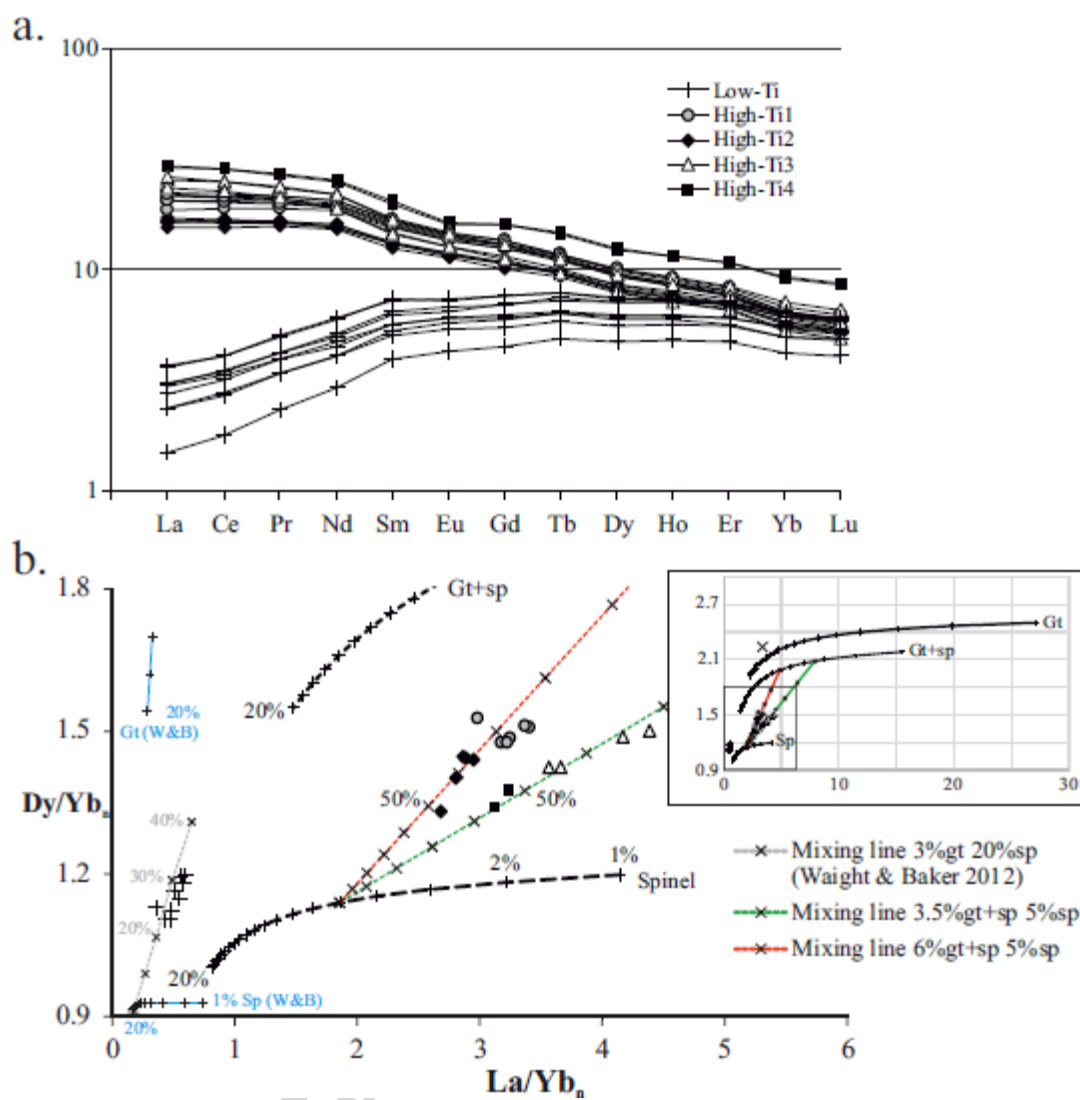Figure 6

Figure 7

Figure 8

1 2 3

Local eruption source

1

2

3

Pre-existing lava field topography

1

2

3

Previous lava flow highs

Laterally discontinuous lava facies

1

2

3
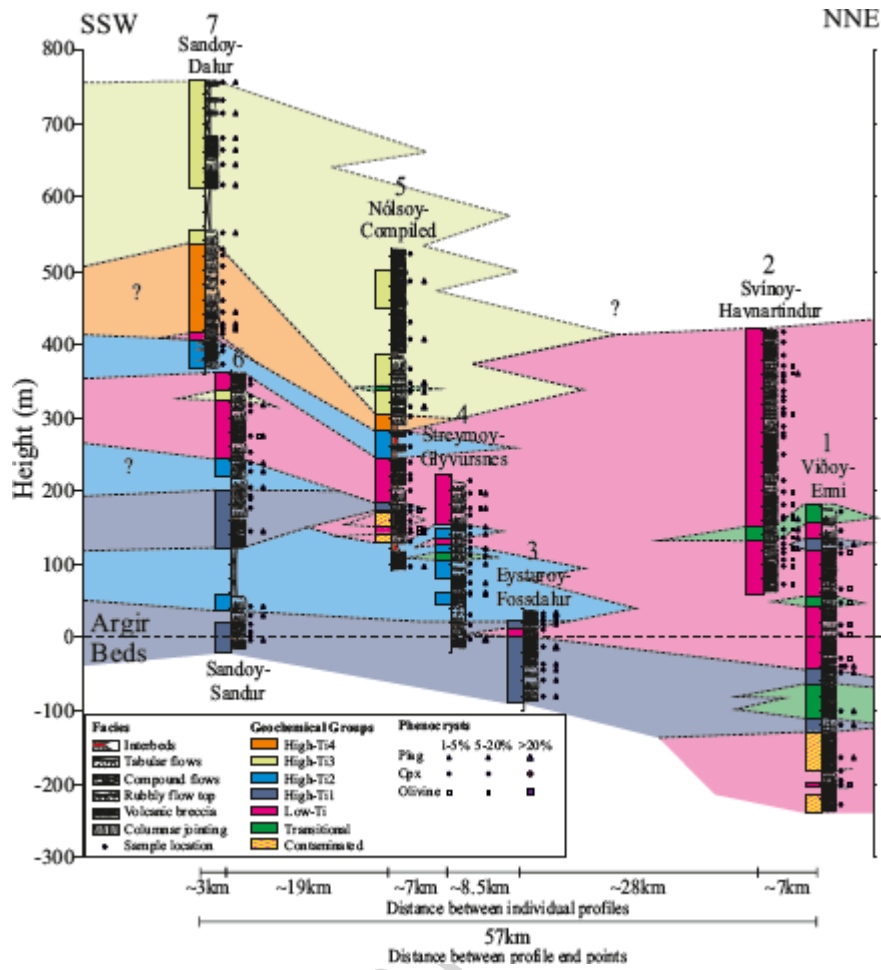
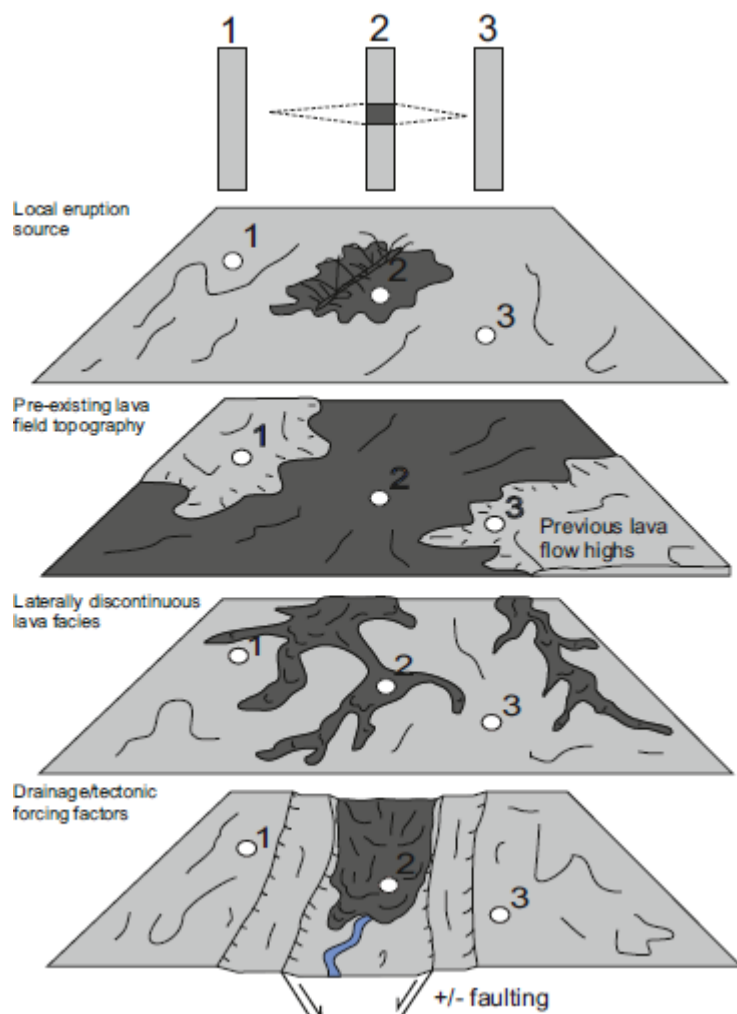Drainage/tectonic forcing factors

1

2
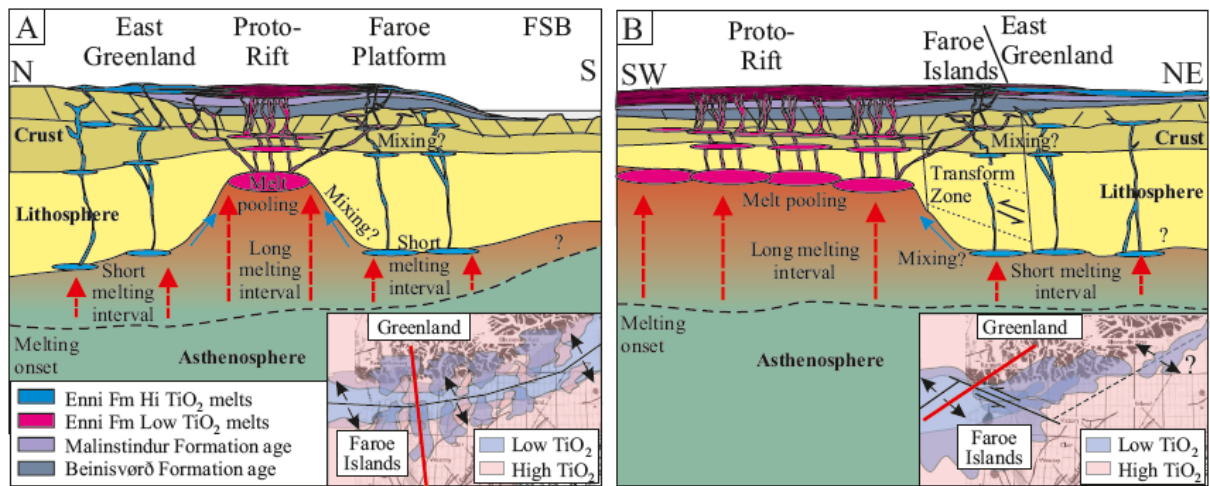
3

+/- faulting

Figure 9

Figure 10

Table 1. Selected XRF major and trace element data and ICP-MS REE data for the main chemical groups.

| Sample | SV12-1-13 | GL-1-16 | SN-3-3 | VD12-1-6 | EY12-1-8 | SN-1-2 | GL-1-8 | SD12-1-1 | NY-1-2 | SD12-1-18 | SD12-1-9 | TJ1-5 | HM1-1 |
|---|---|---|---|---|---|---|---|---|---|---|---|---|---|
| Island | Svínoy | Streymoy | Sandoy (Sandur) | Viðoy | Eysturoy | Sandoy (Sandur) | Streymoy | Sandoy (Dalur) | Nólsoy | Sandoy (Dalur) | Sandoy (Dalur) | Nolsoy (Tjørnunes-1 borehole) | Nolsoy (Høsmøl-1 borehole) |
| Distance to Argir Beds (m) | 215 | 197 | 253 | -164 | 18 | 2 | 100 | 372 | 335 | 680 | 459 | 302 | 338 |
| Group | Low-Ti | Low-Ti | Low-Ti | Low-Ti (contaminated) | High-Ti1 | High-Ti1 | High-Ti2 | High-Ti2 | High-Ti3 | High-Ti3 | High-Ti4 | High-Ti4 | Transitional |
| **XRF majors** | | | | | | | | | | | | | |
| SiO2 | 48.25 | 47.50 | 49.01 | 51.60 | 47.82 | 48.66 | 46.63 | 48.03 | 47.63 | 46.54 | 46.45 | 46.20 | 48.51 |
| TiO2 | 0.99 | 1.10 | 1.41 | 1.02 | 2.86 | 3.05 | 2.43 | 2.46 | 2.82 | 3.25 | 3.92 | 3.93 | 1.63 |
| Al2O3 | 14.86 | 14.82 | 14.15 | 15.70 | 13.92 | 13.84 | 14.76 | 13.60 | 14.70 | 14.49 | 13.00 | 12.74 | 13.72 |
| Fe2O3 | 11.91 | 11.99 | 12.90 | 9.84 | 14.16 | 15.18 | 14.30 | 14.83 | 13.78 | 14.57 | 17.07 | 17.40 | 13.83 |
| MnO | 0.18 | 0.18 | 0.19 | 0.16 | 0.20 | 0.20 | 0.19 | 0.21 | 0.19 | 0.19 | 0.23 | 0.24 | 0.21 |
| MgO | 8.49 | 8.39 | 7.66 | 6.88 | 5.89 | 6.23 | 6.32 | 6.55 | 7.24 | 6.01 | 5.95 | 5.96 | 6.90 |
| CaO | 12.57 | 12.17 | 12.19 | 10.00 | 8.95 | 10.16 | 10.85 | 10.99 | 10.81 | 10.99 | 10.70 | 10.70 | 11.73 |
| Na2O | 1.84 | 1.83 | 1.99 | 2.09 | 3.42 | 2.78 | 2.16 | 2.33 | 2.34 | 2.43 | 2.12 | 2.46 | 2.36 |
| K2O | 0.10 | 0.12 | 0.24 | 0.94 | 0.21 | 0.36 | 0.22 | 0.33 | 0.31 | 0.17 | 0.23 | 0.25 | 0.16 |
| P2O5 | 0.07 | 0.08 | 0.11 | 0.11 | 0.25 | 0.27 | 0.20 | 0.22 | 0.28 | 0.29 | 0.34 | 0.37 | 0.14 |
| LOI | 0.49 | 1.42 | 1.35 | 1.06 | 1.78 | 0.00 | 1.64 | 0.08 | 0.26 | 0.52 | 0.00 | -0.28 | 0.02 |
| Total | 99.74 | 99.61 | 101.19 | 99.40 | 99.45 | 100.75 | 99.70 | 99.64 | 100.35 | 99.44 | 100.01 | 99.97 | 99.21 |
| **XRF traces** | | | | | | | | | | | | | |
| Rb | 1 | 0 | 3 | 10 | 2 | 3 | 3 | 4 | 6 | 1 | 4 | 1.9 | 1 |
| Sr | 102 | 112 | 111 | 181 | 242 | 280 | 235 | 228 | 276 | 316 | 226 | 222 | 169 |
| Y | 26.1 | 25.4 | 32.6 | 24.6 | 36.1 | 37.9 | 32.4 | 33.3 | 30.2 | 35.1 | 49.0 | 49.9 | 29.6 |
| Zr | 53 | 59 | 76 | 99 | 192 | 198 | 151 | 147 | 172 | 199 | 239 | 248.8 | 103.2 |
| Nb | 2.0 | 2.6 | 3.5 | 3.9 | 14.6 | 15.5 | 11.7 | 12.2 | 20.1 | 22.1 | 23.0 | 22.9 | 8.2 |
| Ba | 22 | 19 | 29 | 208 | 78 | 112 | 60 | 68 | 86 | 83 | 89 | 106.6 | 53.9 |
| Pb | 2 | 1 | 3 | 3 | 2 | 4 | 4 | 1 | 3 | 3 | 6 | 9.4 | 4.1 |
| Th | 0 | 2 | 3 | 3 | 2 | 3 | 2 | 3 | 4 | 4 | 3 | 0.6 | 4.4 |
| U | 1 | 0 | 1 | 1 | 2 | 1 | 2 | 2 | 2 | 2 | 3 | 1.4 | 0 |
| Sc | 47 | 46 | 49 | 34 | 35 | 38 | 36 | 43 | 32 | 36 | 43 | 44.4 | 44.2 |
| V | 301 | 300 | 364 | 231 | 399 | 411 | 371 | 382 | 330 | 379 | 476 | 458.9 | 393.8 |
| Cr | 359 | 351 | 266 | 227 | 90 | 150 | 143 | 160 | 225 | 153 | 125 | 138.6 | 156.6 |
| Co | 48 | 43 | 43 | 39 | 35 | 39 | 37 | 43 | 44 | 41 | 40 | 32.8 | 38.7 |
| Ni | 131 | 121 | 114 | 83 | 73 | 94 | 97 | 87 | 133 | 95 | 93 | 86.8 | 87.1 |
| Cu | 148 | 106 | 187 | 77 | 116 | 196 | 206 | 221 | 198 | 253 | 338 | 324.6 | 176.9 |
| Zn | 73 | 69 | 77 | 67 | 101 | 111 | 94 | 102 | 97 | 106 | 130 | 127.7 | 87.8 |
| Ga | 17 | 17 | 18 | 21 | 21 | 24 | 21 | 24 | 22 | 22 | 25 | 23.9 | 19.5 |
| **ICP-MS REE** | | | | | | | | | | | | | |
| La | 1.54 | 1.78 | 2.35 | | 13.34 | 13.89 | 10.53 | 11.08 | 15.12 | 16.96 | 18.57 | 18.99 | 6.59 |
| Ce | 4.63 | 5.31 | 6.81 | | 34.11 | 35.33 | 27.93 | 28.02 | 37.76 | 41.99 | 47.21 | 47.31 | 16.06 |
| Pr | 0.86 | 1.00 | 1.26 | | 5.11 | 5.27 | 4.13 | 4.17 | 5.33 | 6.02 | 6.77 | 6.90 | 2.49 |
| Nd | 5.06 | 5.90 | 7.44 | | 24.13 | 24.88 | 19.23 | 19.36 | 23.62 | 27.20 | 31.02 | 31.81 | 12.08 |

| | | | | | | | | | | | | |
|---|---|---|---|---|---|---|---|---|---|---|---|---|
| **Sm** | 2.17 | 2.31 | 2.99 | 6.46 | 6.56 | 5.30 | 5.32 | 5.87 | 6.86 | 8.09 | 8.31 | 3.55 |
| **Eu** | 0.88 | 0.92 | 1.12 | 2.12 | 2.15 | 1.83 | 1.78 | 1.96 | 2.21 | 2.45 | 2.48 | 1.25 |
| **Gd** | 3.24 | 3.30 | 4.15 | 6.97 | 6.98 | 5.80 | 5.85 | 6.04 | 7.01 | 8.70 | 8.68 | 4.22 |
| **Tb** | 0.62 | 0.62 | 0.78 | 1.11 | 1.14 | 0.95 | 0.96 | 0.94 | 1.11 | 1.42 | 1.45 | 0.76 |
| **Dy** | 4.12 | 4.02 | 5.00 | 6.46 | 6.47 | 5.48 | 5.71 | 5.38 | 6.30 | 8.31 | 8.38 | 4.65 |
| **Ho** | 0.92 | 0.88 | 1.09 | 1.30 | 1.30 | 1.09 | 1.19 | 1.06 | 1.27 | 1.71 | 1.72 | 1.01 |
| **Er** | 2.66 | 2.49 | 3.10 | 3.47 | 3.41 | 3.00 | 3.23 | 2.86 | 3.34 | 4.69 | 4.69 | 2.89 |
| **Yb** | 2.44 | 2.20 | 2.77 | 2.86 | 2.80 | 2.56 | 2.81 | 2.35 | 2.77 | 4.05 | 3.99 | 2.56 |
| **Lu** | 0.35 | 0.33 | 0.40 | 0.40 | 0.40 | 0.36 | 0.40 | 0.33 | 0.39 | 0.58 | 0.58 | 0.38 |

**Table 2. Chemical criteria used for distinguishing the separate chemical groups within this study.**

| Chemical group | Distinguishing criteria |
|---|---|
| Low-Ti | Zr/Y < 2.6, TiO2 < 1.5 wt% and La/Smn <0.6. |
| High-Ti1 | Zr/Nb 12.1-15, Nb/Y 0.34-0.43, Zr/Y 4.95-5.4 and TiO2 2.7-3.8 wt% |
| High-Ti2 | Zr/Nb 10.4-13.3, Nb/Y 0.34-0.43, Zr/Y 4.4-5 and TiO2 2-2.6 wt% |
| High-Ti3 | Zr/Nb 8.5-10.6, Nb/Y 0.47-0.66, V < 420ppm and TiO2 2.8-3.6 wt% |
| High-Ti4 | Zr/Nb 9.8-10.9, Nb/Y 0.45-0.52, V > 450ppm and TiO2 3.79-4 wt% |

**Highlights**

- New stratigraphically constrained major and trace element data from the Enni Formation of the Faroe Islands are presented

- One Low-Ti and four High-Ti melt groups are identified based on trace element signatures and linked to the East Greenland stratigraphy

- Chemical correlation potential in large igneous provinces is strongly affected by facies architecture

- Non-uniform lithospheric thinning during continental rupture may have delayed the onset of Low-Ti melting between the Faroe Islands and East Greenland